J. Fluid Mech. (1991), *vol.* 226, *pp.* 475–496
Printed in Great Britain

Flow of non-Newtonian fluids over a confined baffle

F. T. PINHO AND J. H. WHITELAW
Imperial College of Science, Technology and Medicine, Department of Mechanical Engineering, Fluids Section, Exhibition Road, London SW7 2BX, UK

(Received 22 February 1990 and in revised form 24 August 1990)

Measurements of wall pressure, and mean and r.m.s. velocities of the confined flow about a disk of 50% area blockage have been carried out for two Newtonian fluids and four concentrations of a shear-thinning weakly elastic polymer in aqueous solution encompassing a Reynolds-number range from 220 to 138000. The flows of Newtonian and non-Newtonian fluids were found to be increasingly dependent on Reynolds numbers below 50000, with a decrease in the length of the recirculation region and dampening of the normal Reynolds stresses. At Reynolds numbers less than 25000, the recirculation bubble lengthened and all turbulence components were suppressed with increased polymer concentration so that, at a Reynolds number of 8000, the maximum values of turbulent kinetic energy were 35 and 45% lower than that for water, with 0.2% and 0.4% solutions of the polymer. Non-Newtonian effects were found to be important in regions of low local strain rates in low-Reynolds-number flows, especially inside the recirculation bubble and close to the shear layer, and are represented by both an increase in viscous diffusion and a decrease in turbulent diffusion to, respectively, 6% and 18% of the largest term of the momentum balance with a 0.4% polymer solution at a Reynolds number of 7700. The asymmetry and unsteadiness of the flow at Reynolds numbers between 400 and 6000 is shown to be an aerodynamic effect which increases in range and amplitude with the more concentrated polymer solutions.

1. Introduction

The results presented here were obtained in the flow downstream of a baffle located on the axis of a round duct with a range of concentrations of sodium carboxy methyl cellulose (CMC) in water. The geometrical arrangement is similar to that investigated by Taylor & Whitelaw (1984) with water and by Nouri, Whitelaw & Yianneskis (1987) with dense two-phase flows. The experiments were undertaken to determine the influence of non-Newtonian behaviour on a flow with large-scale recirculation and are relevant to mixing processes such as those in stirred tanks, see for example Yianneskis, Popiolek & Whitelaw (1987).

Information on non-Newtonian free shear layer flows is relevant to this work but the little available in the literature is restricted to dilute polymer solutions of constant viscosity and does not allow unambiguous conclusions. White (1967) reported an increase of the angle of spread of an axisymmetric jet with polyethylene oxide, but not with other polymer solutions, and Barker (1973) showed that initial conditions are important with non-Newtonian fluids. For a mixing layer, Kwade (1982) reported an enhancement of the intensity and coherence of large turbulent

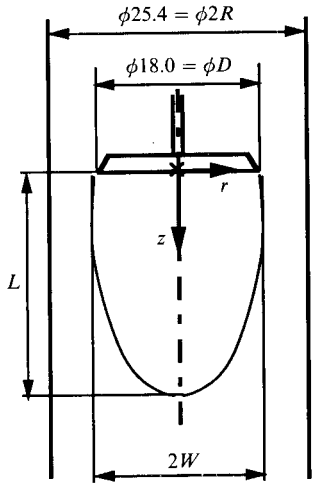

FIGURE 1. Test section and relevant parameters.

eddies while microstructures were attenuated, and the more recent investigation of axisymmetric jets by Koziol & Glowacki (1989) has shown damping of turbulent fluctuations especially in the transverse direction.

Detailed information of separated flows of non-Newtonian fluids is scarce and usually related to low Reynolds numbers. Adachi, Yoshioka & Sakai (1977/78), for example, showed that the flow of a shear-thinning fluid over a sphere resulted in a decrease of friction and pressure drag and an increase in the size of the vortices, but the experiments were confined to Reynolds numbers less than sixty. Mena, Manero & Leal (1987) conducted similar experiments with flows around confined spheres and showed that shear-thinning and elasticity led to reduced influence of the confining wall, but the Reynolds numbers were less than ten. Consequently, numerical investigations such as that of Dairenieh & McHugh (1985) are restricted in their applicability by the available physical knowledge. In a more recent investigation, Pinho & Whitelaw (1988) reported measurements in the flow of a shear-thinning fluid downstream of a baffle and achieved a Reynolds number of 5600 for which they confirmed the existence of periodic fluctuations, but these appeared to depend on Reynolds number rather than on the non-Newtonian nature of the fluid.

The reference to Reynolds number with non-Newtonian fluids implies the use of an effective viscosity which introduces uncertainty into comparisons. It is, however, evident that previous experiments have been confined to comparatively low Reynolds numbers and certainly less than those which might be encountered in many practical stirred vessels. Thus, the present investigation was undertaken to compare the velocity characteristics of the flow downstream of a confined baffle with four concentrations of CMC in water and for a near-constant bulk-flow velocity, which gave rise to Reynolds numbers from 7650 to 42300. Experiments were also performed with water and Newtonian solutions of glycerol in water, to provide a range of Reynolds numbers similar to that of the non-Newtonian flows.

The following section describes the flow configuration, measurement techniques and the properties of the fluids, and the results are presented in the third section where mean flow characteristics are considered first. In §4, the roles of a variable viscosity and elasticity on mean and turbulent flow fields and the effects of shear-thinning intensity are discussed and the findings put into context with previous work

with the same fluids in stirred vessels. These results also provide information useful in the evaluation of numerical solutions of the equations of motion which use rheological and turbulence models. The paper ends with a summary of the more important conclusions.

2. Flow configuration, instrumentation and fluid properties

The baffle arrangement is shown in figure 1 together with the coordinate system. The 25.4 mm inside-diameter pipe was located with its axis vertical. Fluid was pumped from a 60 l tank to the top of the closed circuit, through 90 diameters of the pipe to the transparent acrylic test section and through a further 30 diameters to the tank. The flow was controlled with two valves and the velocity and pressure drop measurements monitored the flow rate within 10% from day to day. A 75 mm length of honeycomb and a 20 mm inside-diameter ring were located at the entrance to the straight pipe. The test section had a square outer cross-section and was polished on its outer and inner surfaces. The 0.5 area-blockage disk was secured on the axis with uncertainty of less than 0.015 mm by four streamlined pylons of maximum width 1.0 mm and their trailing edges were located 40 maximum thicknesses upstream of the plane of the disk. Six static-pressure holes of 0.5 mm diameter were arranged along the test section.

The results include profiles of single-point measurements of three components of velocity and the static-pressure distribution along the pipe wall. The velocity information was obtained with a laser velocimeter operated with forward-scattered light and with signals processed by a counter. Details of the optical and signal processing systems and of the pressure transducer are given by Pinho & Whitelaw (1990). Maximum uncertainties in mean and r.m.s. velocities were 1.5% and 7% respectively and 3% in the pressure measurements with a 95% level of confidence. For present purposes, it is important to indicate that the flow in the test section in the absence of the baffle gave rise to a linear pressure distribution for all flows considered here and that the dimensions of the measuring volume of the velocimeter gave rise to gradient-broadening effects only in the immediate vicinity of the pipe wall.

The choice of a non-Newtonian, weakly elastic, shear-thinning fluid was made after consideration of the properties of a wider range of fluids, and the Appendix provides a brief account of the investigation which led to the choice of CMC. The relationship between shear rate and stress of four aqueous solutions of CMC is shown in figure 14 and their viscosities were found to decrease by less than 10% after stresses were exerted on the fluid inside the baffle rig for 6 h, the time limit used in the fluid dynamic experiments. The effective viscosity was calculated for a shear rate, defined as

$$\dot{\gamma} = \left[\frac{U_{\max} - U_{\min}}{\Delta r}\right]_{\max}, \tag{1}$$

which represents an average value in the recirculation and shear layer regions in a plane close to the centre of the recirculation bubble. $U_{\max}$ and $U_{\min}$ are the maximum positive and negative velocities in the annular jet and recirculation regions and Δr is the radial distance between them. The viscosity values obtained from this definition and the relationships of figure 16 together with the diameter of the disk and the bulk-flow velocity in the annulus formed the Reynolds numbers (Re_b) quoted in tables and figures. Another Reynolds number (Re_c), defined with a flow-field-

Fluid	U_0(m/s)	$Re_b(Re_c)$	L/D	W/D	U_i/U_0	U_r/U_0	$\dot{m}_r/\dot{m}$
Water	7.68	138000	2.05	0.54	1.29	−0.62	−0.22
Water	1.27	22800	1.94	0.53	1.28	−0.60	−0.23
Glyc. and water	6.52	11600	1.77	0.52	1.26	−0.61	−0.20
Glyc. and water	4.6	8180	1.57	0.52	1.24	−0.55	−0.19
0.1% CMC	8.88	42300 (41400)	1.92	0.53	1.26	−0.58	−0.22
0.2% CMC	8.94	22700 (21100)	1.93	0.54	1.24	−0.57	−0.22
0.2% CMC	4.09	8250 (7940)	1.85	0.52	1.26	−0.54	−0.18
0.3% CMC	8.69	12130 (11560)	2.01	0.53	1.25	−0.55	−0.19
0.4% CMC	8.40	7650 (7360)	2.16	0.53	1.22	−0.53	−0.18

TABLE 1. Some mean-flow characteristics

independent viscosity at a shear rate equal to the ratio of annular bulk velocity to the pipe-baffle diameter gap, is quoted in table 1 between brackets.

Table 1, lists some mean-flow characteristics of the flows considered here and shows that the Reynolds number decreased with increasing concentrations of CMC. To separate the effects of the non-Newtonian fluids from those of Reynolds number, the experiments included the use of Newtonian fluids based on aqueous solutions of glycerol. A 53.2% by volume solution of glycerol in water, for example, had a density, kinematic viscosity and refractive index of 1142 kg/mm^3, 10.1 cS and 1.4135 respectively at 20.5 °C.

3. Results

Values of axial mean velocity are presented on figures 2 and 3 for water and aqueous solutions of CMC, and figure 2 includes values of the pressure coefficient based on wall values of pressure and relative to the baffle plane. The pressure and the centreline distributions of axial velocity differ by less than 25% of the maximum values although the Reynolds number varies by a factor of twenty and the axial velocities, normalized by the annular jet bulk velocity, differ by less than 10%. The trends of the results can be attributed to the combined effects of fluid and Reynolds number and additional measurements with Newtonian fluids at low Reynolds numbers similar to those of 0.2, 0.3 and 0.4% CMC were obtained to separate the effects. For example, the Newtonian fluid centreline profiles of axial mean velocity of figure 4 show a variation of bubble length of the order of 25% as the Reynolds number changes from 138000 to 8000.

Table 1 quantifies the length (L) and width (W) of the recirculation region, normalized by the baffle diameter (D), the maximum negative and positive values of the axial velocity component U_r and U_j respectively, normalized by the annular bulk velocity (U_0) and the ratio of recirculation mass flow rate ($\dot{m}_r$) to the total mass flow rate ($\dot{m}$) obtained by numerical integration of the mean velocity profiles. Since the viscosity of a non-Newtonian fluid varies with the local flow properties the use of an effective value in a Reynolds number implies simplification. Two typical Reynolds numbers are, therefore, quoted. Re_c is independent of the flow field and consequently has a more universal character facilitating comparisons with other investigations, but lacks physical meaning in terms of the flow under investigation. The effective viscosity used in Re_b corresponds to the discussion of the previous section and is based on the shear layer between the annular jet and bubble, where the highest shear rates will result in the lowest viscosities, and the centreline region where the opposite

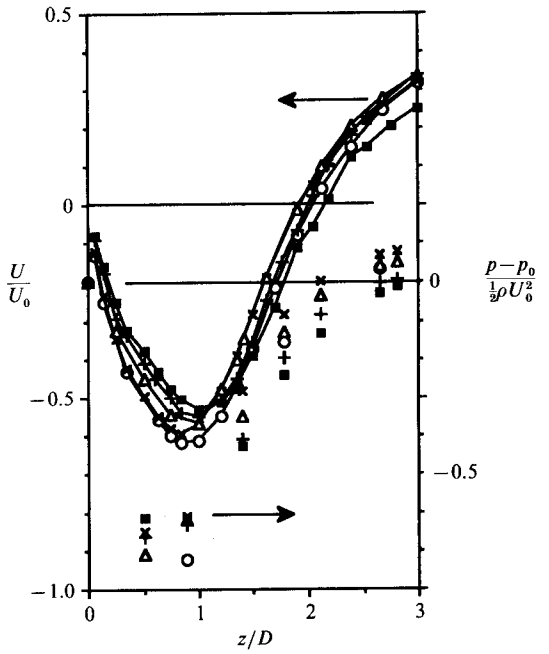

FIGURE 2. Pressure coefficient and centreline axial mean velocity profile (——). ○, water; ×, 0.1% CMC; Δ, 0.2% CMC; +, 0.3% CMC; ■, 0.4% CMC.

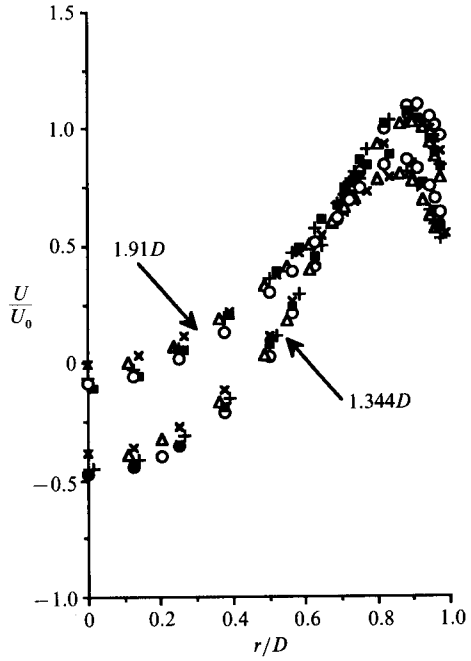

FIGURE 3. Axial mean velocity profiles at 1.344D and 1.91D downstream of baffle plane for maximum flow rate. ○, Water-Re = 138000; ×, 0.1% CMC-Re = 42300; △, 0.2% CMC-Re = 22700; +, 0.3% CMC-Re = 12130; ■, 0.4% CMC-Re = 7650.

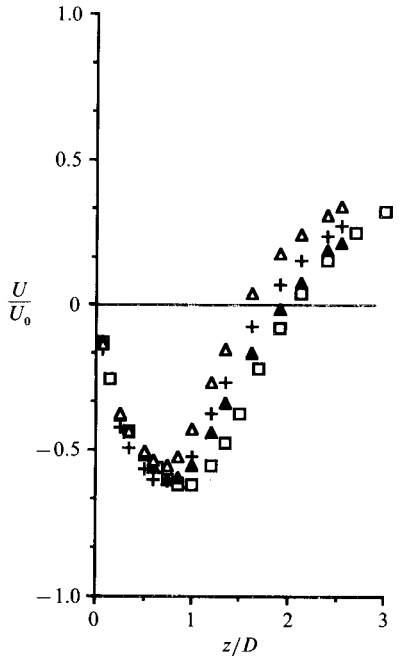

FIGURE 4. Newtonian centreline mean axial velocity profile: □, $Re = 138000$; ▲, $Re = 22800$; +, $Re = 11600$; △, $Re = 8200$.

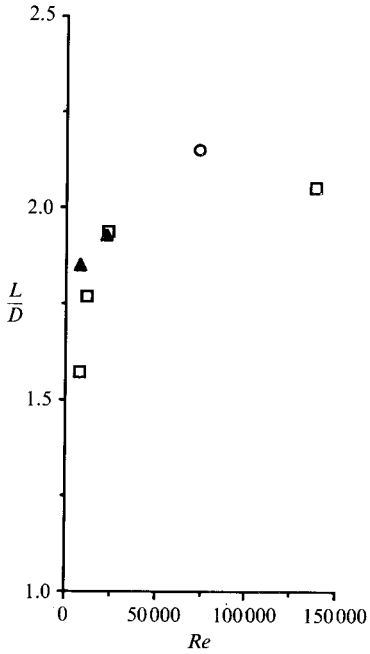

FIGURE 5. Normalized bubble length for □, Newtonian and ▲, 0.2% CMC as function of Reynolds number; ○ is from Nouri (1988).

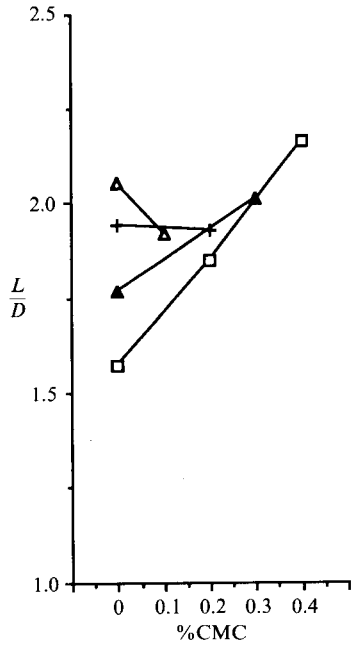

FIGURE 6. Normalized bubble length as function of polymer concentration: □, $Re = 8000$; ▲, $Re = 12000$; +, $Re = 22700$; △, $Re = 42300$; ×, $Re = 136000$.

occurs. There are clear limitations to this definition which, for instance, does not take account of the viscosities involved in the high-frequency fluctuations characteristic of the viscous dissipation process.

The length of the recirculation bubble increases directly with Reynolds number for both Newtonian and non-Newtonian fluids as shown in figure 5, where the 0.2% CMC solution represents the shear-thinning fluids and Newtonian data from other sources were included. The changes in bubble length are restricted mainly to Reynolds numbers below 40000 and there seems to be no change in bubble size for higher values, as far as the Newtonian fluids are concerned. It is possible, however, that higher Reynolds numbers will lead to further changes for concentrated polymer solutions because of their tendency to extend transition regimes and delay turbulence, as reported by Pinho & Whitelaw (1990) for the pipe flow. The effects of polymer concentration, figure 6, are more complex since the trends observed in the variation of bubble length also depend on Reynolds number. At low and constant Reynolds numbers the recirculation size increases with polymer concentration whereas, for Newtonian fluids, it increases with Reynolds number.

The high viscosity of the more concentrated polymer solutions did not allow high-Reynolds-number flows to be achieved, therefore restricting the extension of the comparisons but, if the effects of Reynolds number on 0.3% and 0.4% CMC are similar to that observed for the 0.2% CMC solution, then figure 6 would show that an increase in polymer concentration would increase bubble length at high Reynolds number, whereas the addition of small quantities of polymer to a Newtonian solvent would reduce its size. The width of the bubble was obtained from the calculation of the streamlines and the changes are too small to be significant (within 5%), because the high mean-flow kinetic energy of the annular jet constrains the bubble width.

The characteristic velocities of the recirculation bubble (U_r) and annular jet (U_j)

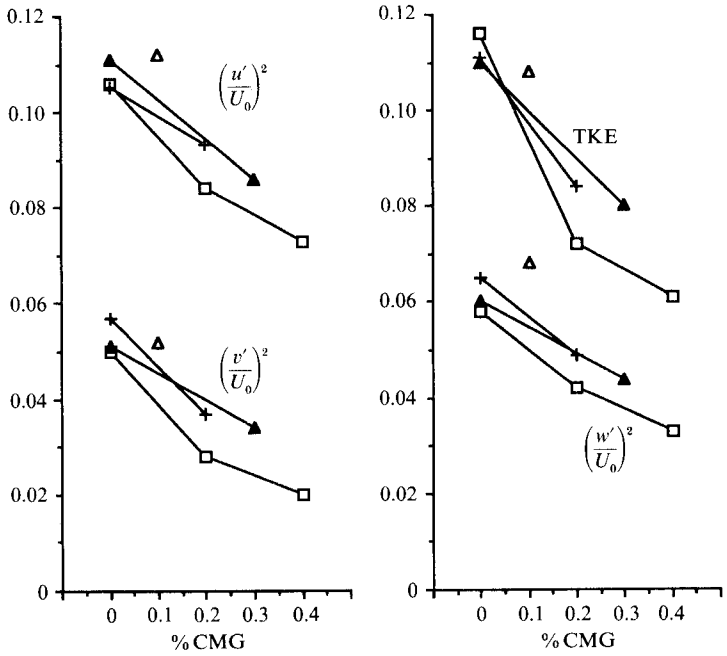

FIGURE 7. Maximum values of normal Reynolds stress and turbulent kinetic energy as a function of concentration: □, $Re = 8000$; ▲, $Re = 12000$; +, $Re = 22700$; △, $Re = 42300$.

Fluid	Re_b	$\left(\frac{u'^2}{U_0^2}\right)_{max}$	$\left(\frac{v'^2}{U_0^2}\right)_{max}$	$\left(\frac{w'^2}{U_0^2}\right)_{max}$	TKE_{max}
Water	138000	0.110	0.059	0.074	0.116
Water	22800	0.105	0.057	0.065	0.111
Glyc. and water	11600	0.111	0.051	0.060	0.110
Glyc. and water	8180	0.106	0.050	0.058	0.116
0.1% CMC	42300	0.112	0.052	0.068	0.108
0.2% CMC	22700	0.093	0.037	0.049	0.084
0.2% CMC	8250	0.084	0.028	0.042	0.072
0.3% CMC	12130	0.086	0.034	0.044	0.080
0.4% CMC	7650	0.073	0.020	0.033	0.061

TABLE 2. Some turbulent flow characteristics: TKE = turbulent kinetic energy

decrease with Reynolds number for both Newtonian and non-Newtonian fluids and also with the increase in polymer concentration at constant Reynolds number. This means that the magnitudes of the favourable pressure gradient in the annular jet and of the adverse pressure gradient behind the disk also become lower, with the reduction in the ratio of recirculation to total mass flow rates indicating a higher reduction of the latter.

The turbulent quantities corresponding to the flows of table 1 are summarized in table 2 and show that the maximum normal stresses decrease with Reynolds number by up to 20%, corresponding to 10% in intensity. The effect of the non-Newtonian fluid is much greater, however, with reductions up to 60% at the same Reynolds number and proportionally greater damping of the radial and tangential components as shown in figure 7. The variations of radial and circumferential turbulent quantities

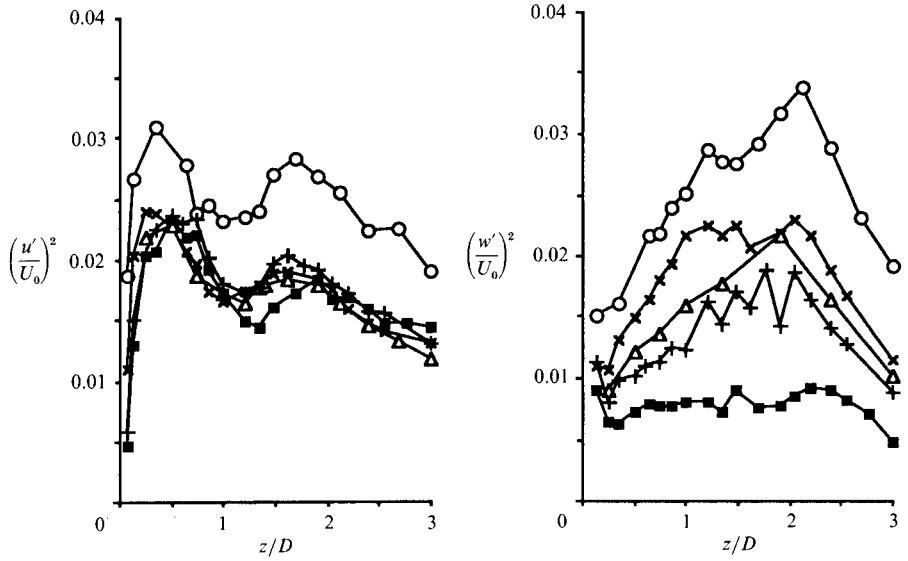

FIGURE 8. Normalized centreline profiles of axial and tangential normal Reynolds stress; ○, water ($Re = 138000$); ×, 0.1% CMC ($Re = 42300$); △, 0.2% CMC ($Re = = 22700$); +, 0.3% CMC ($Re = 12130$); ■, 0.4% CMC ($Re = 7650$).

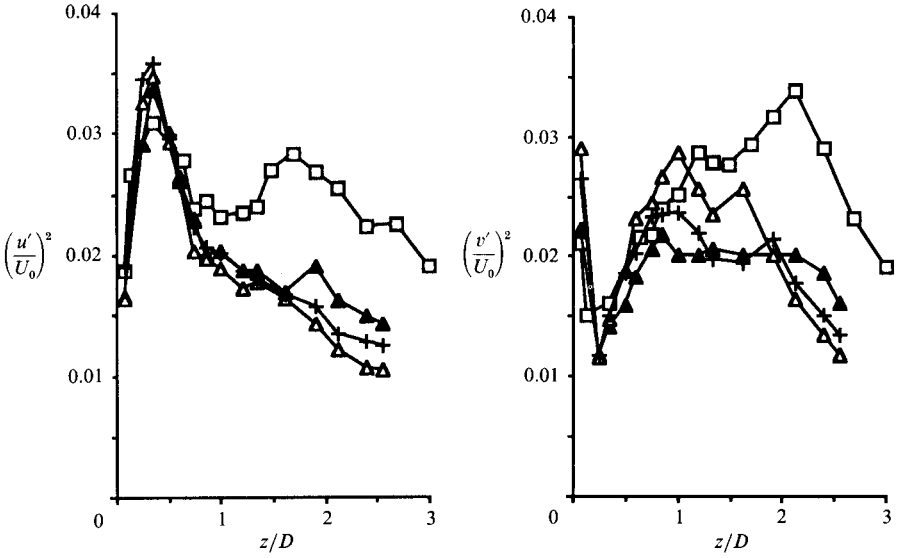

FIGURE 9. Newtonian centreline profiles of normalized axial and radial normal Reynolds stress: □, $Re = 138000$; △, $Re = 22800$; +, $Re = 11600$; ▲, $Re = 8200$.

with polymer concentration are everywhere proportional to their maximum values, with variations of the axial component of smaller magnitude and confined to the shear layer region.

The centreline distributions of the axial and cross-stream normal Reynolds stresses of figure 8 correspond to the mean velocity profiles of figure 2, and show reductions with increasing CMC concentration and decreasing Reynolds numbers. The maximum axial stresses are similar in magnitude but around 25% lower than

with water, and the cross-stream values decrease much more rapidly than do the longitudinal fluctuations with increasing CMC concentration. These results may be compared with those of figure 9 obtained with Newtonian fluids and corresponding to the mean velocities of figure 4. The effects of the non-Newtonian fluids and of Reynolds number are not the same in that a decrease of Reynolds number for Newtonian fluids is accompanied by a strong reduction of turbulence intensity near the rear stagnation point but not upstream, whereas for the CMC solutions the axial component is barely affected but the transverse component is everywhere attenuated.

4. Discussion

The shear-thinning viscosity and elasticity of non-Newtonian solutions can affect the transport of mean momentum and turbulent energy in turbulent flow, and the high viscosity normally associated with these fluids limits the maximum achievable Reynolds number. The following paragraphs assess the importance of those effects on mean-flow properties and on turbulence, relative to Newtonian fluids. Reynolds-number and concentration effects are also investigated, with the former effect analysed for Newtonian fluids.

The influence of a shear-thinning viscosity on mean flow characteristics can be investigated by an order of magnitude analysis of the extra terms of the mean momentum equation. Assuming that the total viscosity ($\hat{\mu}$) of a non-Newtonian fluid at a particular strain rate is the sum of an average value (μ), equal to the viscosity at the average strain rate ($S_{ij} = \partial u_i/\partial x_j$), and a viscosity of the fluctuating flow (μ') with *non-zero* average value ($\overline{\mu'}$), the difference between the Newtonian and non-Newtonian mean momentum equation is the two new diffusion terms that contain fluctuations of viscosity, as shown in equation (2):

$$\frac{\partial(2\mu S_{ij} + 2\overline{\mu' s_{ij}} + 2\overline{\mu'} S_{ij} - \rho\overline{u_i u_j})}{\partial x_j}, \tag{2}$$

To calculate the ratio of the two non-Newtonian terms to the Newtonian term ($2\mu S_{ij}$), the viscosity was represented by an Ostwald–De Waele power-law function and expanded into a Taylor series. Two possible relationships between the intensity of the fluctuations of strain rate (s_{ij}) and its average value (S_{ij}) were investigated: $(\overline{s_{ij}^2})^{\frac{1}{2}}$ much higher than $|S_{ij}|$, which corresponds to the situation normally found in turbulent flow; and, because of the high viscosity at low Reynolds numbers, $|S_{ij}| \gg (\overline{s_{ij}^2})^{\frac{1}{2}}$. The results are shown in table 3 where μ_∞ and μ_0 are respectively the viscosity at the limits of infinite and zero shear rate and n is the index of the viscosity power law. For shear-thinning fluids $\mu_\infty < \mu_0$ and $n < 1$ and the terms containing the viscosity fluctuations are at most of the same magnitude as the average viscosity diffusion term and always of opposite sign, so that the addition of all viscous diffusion terms is roughly equivalent to a single viscous diffusion term of lower average and constant viscosity. Thus, the variation of viscosity cannot explain the differences between Newtonian and polymer solutions of the previous section, and they must be the result of another property such as elasticity.

Mean-flow characteristics change for Reynolds numbers less than 40000 and the reduction of the ratio of inertial to viscous forces gives rise to slightly narrower and shorter recirculation bubbles with smaller recirculating mass flow rates. The direct proportionality between maximum negative centreline velocity, recirculation mass flow rate, bubble length and pressure gradients discussed by Taylor & Whitelaw (1984) for high-Reynolds-number flows is still valid over this range so that a

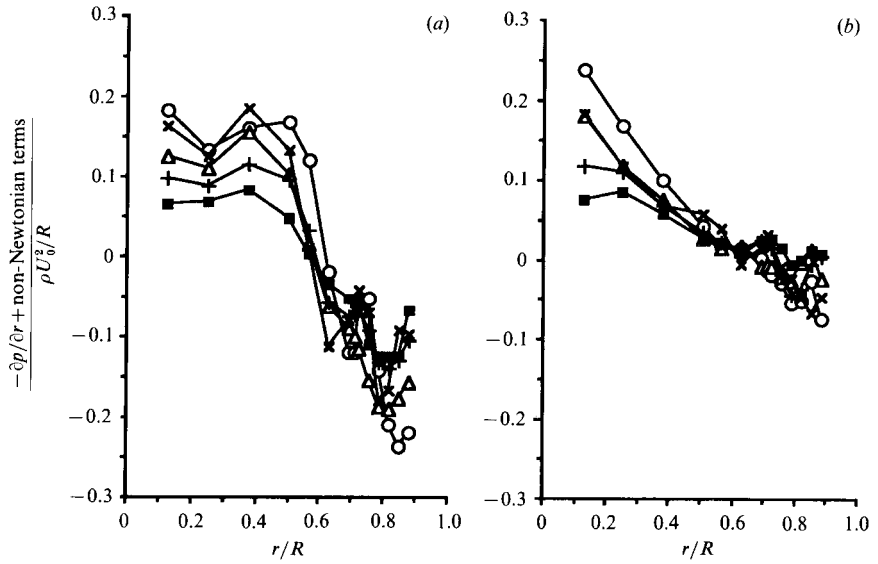

FIGURE 10. Radial profiles of the sum of the radial gradient of pressure and the non-Newtonian terms of the radial momentum equation: ○, water; ×, 0.1% CMC; △, 0.2% CMC; +, 0.3% CMC; ■, 0.4% CMC. (*a*) 1.0*D*, (*b*) 1.91*D*.

Terms	$\lvert S_{ij}\rvert \ll (\overline{s_{ij}^2})^{\frac{1}{2}}$		$\lvert S_{ij}\rvert \gg (\overline{s_{ij}^2})^{\frac{1}{2}}$
Momentum equation	-1	to 0	0
$\dfrac{-2\overline{\mu' S_{ij}}}{2\mu S_{ij}}$	(low $\lvert S_{ij}\rvert$)	(high $\lvert S_{ij}\rvert$)	
Momentum equation	$-1 < n-1$	to $(n-1)\dfrac{\mu_\infty}{\mu_0} < 0$	0
$\dfrac{-2\overline{\mu' s_{ij}}}{2\mu S_{ij}}$	(high $\lvert S_{ij}\rvert$)	(low $\lvert S_{ij}\rvert$)	

TABLE 3. Results of the order of magnitude analysis of some momentum equation terms

reduction in Reynolds number leads to results similar to those obtained with a change in baffle geometry from disk to cone, i.e. to a decrease of body bluffness.

The terms of the mean momentum equation help to clarify some aspects of non-Newtonian low-Reynolds-number flows and, with the exception of non-Newtonian viscous diffusion, these were calculated with the pressure gradient obtained by addition. According to Taylor & Whitelaw (1984), the distribution of normal Reynolds stresses is similar to that of a simple mixing layer and this was assumed for the Reynolds shear stress. For the water flow, the term $\overline{u'v'}/U_0^2$ was assumed to vary linearly from zero at the centreline to a maximum of 0.015 at the shear layer ($r/R = 0.71$) and to zero at the annular jet ($r/R = 0.88$), with the maximum value based on measurements of Fujii, Gomi & Eguchi (1978) with a confined flat plate of 50% area blockage. The Reynolds shear stress in the polymer solution flows was assumed to be dampened in proportion to $(\overline{u'^2}+\overline{v'^2})$.

The flow downstream of the rear stagnation point is characterized by the recovery of the mean velocity so that, at three baffle diameters downstream of the disk and

for the water flow at a Reynolds number of 138000, the pressure gradient contribution to momentum change varies from about 95% on the centreline to 50% of the inertia term at $r/R = 0.8$ to 0.9, after passing through zero at $r/R = 0.55$, with the turbulent diffusion accounting for the remainder. The combined influence of polymer concentration and Reynolds number is observed in the slower rate of recovery of the flow of a 0.4% CMC solution for the same mass flow rate as for the water flow and, because of the lower turbulence, the contribution of pressure gradient to momentum exchange is some 65% at $r/R = 0.8$ to 0.9 at the expense of a decrease in turbulent diffusion to 30%. The average viscous diffusion contribution increased from a negligible 0.05% to about 2% to 4% with the reduction in Reynolds number from 138000 to 7650 because, with the low local strain rates, the viscosities are higher than those used to calculate the Reynolds number with the polymer solution.

Between the rear stagnation point ($1.91D$) and the middle of the bubble at $1.0D$, the pressure force is the most important term in a region between the centreline and $r/R = 0.7$, whereas the inertia term is the largest in the annular jet. The contributions of inertia, turbulent diffusion and average viscous diffusion to the pressure gradient force in the central region of the pipe at $1.91D$, are 45%, 55% and 0.02% with the water flow and of 55%, 43.5% and 1.5% with the 0.4% CMC flow. In the annular jet, however, the two thirds of the momentum exchange due to the pressure gradient in the water flow is increased to 75% with the CMC solution, because of a reduction of the turbulent diffusion to 23% and an increase of the average viscous diffusion contribution from under 0.1% to 2%. The same trends were observed at $1.344D$ where turbulent diffusion is less important than at $1.91D$, with contributions never exceeding 20% for the water flow and 30% lower with the 0.4% CMC flow for which the average viscosity diffusion was less than 1%.

Between the disk and the middle bubble plane and inside the recirculation zone, inertia is balanced by the pressure gradient with turbulent diffusion accounting for less than 20% at $0.5D$ and between 35% and 50% at $0.75D$ with the water flow. Turbulence diffusion is two to three times lower with the 0.4% CMC because of the lower turbulence intensity, and the contribution of average viscous diffusion is around 1% and 5% at $0.5D$ and $0.75D$ respectively. In the mid-plane of the bubble ($1.0D$), the main differences between water and the 0.4% CMC solution flows are found inside the recirculation region close to the shear layer, where the ratio of average viscous to turbulent diffusion increases from under 0.5% to about 30%, which corresponds to a variation of 0.1% to 6% in the contribution of viscous diffusion to the pressure gradient, the largest term.

Although the contribution of the viscosity fluctuations reduces the overall importance of viscous diffusion, the results show that, for concentrated polymer solutions at low Reynolds numbers, contributions to diffusion should not be neglected and that, inside the recirculation bubble and other locations where strain rates are small, the effective viscosity will be much higher than the value used in the Reynolds number and laminarization of the flow may occur. The viscometric viscosity is, therefore, important in local regions of low-Reynolds-number flows of strong shear-thinning fluids and in particular its role is emphasized by the large reduction of turbulent diffusion caused by the damping of Reynolds stresses that occurs with non-Newtonian fluids inside the recirculation region and close to the shear layer. The rheological tests of the Appendix did not reveal elasticity with the 0.4% CMC solution, but the pipe flow experiments of Pinho & Whitelaw (1990) show reductions in the turbulent flow friction coefficient of up to 60% with all CMC

Terms	$\lvert S_{ij}\rvert \ll (\overline{s_{ij}^2})^{\frac{1}{2}}$			$\lvert S_{ij}\rvert \ll (\overline{s_{ij}^2})^{\frac{1}{2}}$
TKE equation $\dfrac{-2\overline{\mu' s_{ij}} S_{ij}}{-2\mu \overline{s_{ij}^2}}$	0			$n-1$
TKE equation $\dfrac{-2\overline{\mu' s_{ij}^2}}{-2\mu \overline{s_{ij}^2}}$	-1 (low $\lvert S_{ij}\rvert$)	to	0 (high $\lvert S_{ij}\rvert$)	0

TABLE 4. Results of the order of magnitude analysis of some TKE equation terms

solutions together with a strong damping of turbulence. If it is accepted that drag reduction is due to molecular deformation and the consequent large increase of elongational viscosity, as reported by Berman (1978), the ratio of viscous diffusion to momentum change calculated above will be increased by the contribution of elongational viscosity for all the CMC solutions.

Radial profiles of the calculated radial pressure gradient normalized by $\rho U_0^2/R$ are shown in figure 10 for all fluids at the conditions of figure 3 at planes at the middle ($1.0D$) and end of the recirculation bubble ($1.91D$). The monotonic decrease of $\partial p/\partial r$ observed with polymer concentration is the outcome of a reduction in radial normal Reynolds stress and, if put together with the wall pressure profile of figure 2, there is a reduction in the axial pressure gradient, in particular of the adverse axial pressure gradient in the recirculation zone, which is intensified by a rise in polymer concentration. The increase in bubble length with polymer concentration is, therefore, a consequence of the deterioration of radial momentum exchange which makes the flow around the recirculation region more able to resist an adverse pressure gradient. This happens in spite of a reduction in Reynolds numbers and lower adverse pressure gradients as concentration rises, factors that would tend by themselves to shorten the bubble as is the case with Newtonian fluids.

The turbulent kinetic energy equation is affected by shear-thinning behaviour as an order of magnitude analysis again shows. Two new terms are introduced into the diffusion term (equation (3)) by the viscosity fluctuations and another two into the viscous dissipation (equation (4)) term, so that diffusion and dissipation are:

$$\frac{\partial}{\partial x_j}\left[\frac{1}{2}\rho\overline{u_i u_i u_j} - 2\mu\overline{u_i s_{ij}} - 2\mu\overline{\mu' u_i} S_{ij} - 2\overline{\mu' u_i s_{ij}}\right] \tag{3}$$

and

$$-2\mu\overline{s_{ij}^2} - 2\overline{\mu' s_{ij}^2} - 2\overline{\mu' s_{ij}} S_{ij}. \tag{4}$$

For Newtonian fluids the viscous dissipation is more important than the viscous diffusion term at high Reynolds numbers and only those terms were investigated, with the results presented in table 4. The contribution of viscosity fluctuations can be as important as that of the average viscosity terms but of opposite sign, therefore reducing the amount of dissipation.

With Newtonian fluids, Reynolds numbers less than 40000 lead to smaller values of maximum radial and tangential turbulence intensity but not of the axial component. In the vicinity of the rear stagnation point, the production of turbulence by normal strain–normal stress interaction is much reduced and the peak turbulence found there at high Reynolds numbers disappears, therefore causing low-Reynolds-number baffle flows to resemble a mixing layer. With polymer solutions, however, the

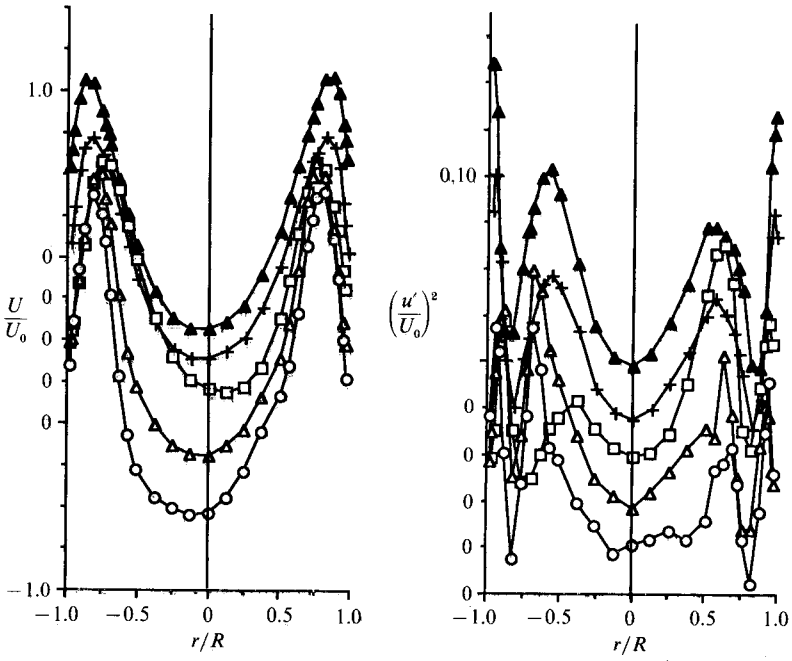

FIGURE 11. Diametral profiles of axial mean velocity and normal Reynolds stress for Newtonian fluids at station $1.0D$ and as a function of Reynolds number: ▲, $Re = 8200$; +$Re = 6310$; □, $Re = 2130$; △, $Re = 1010$; ○, $Re = 540$.

effects of a reduction in Reynolds number are more intense with damping of all three normal Reynolds stresses and by a larger amount than with Newtonian fluids. The damping observed with the non-Newtonian fluids may be due to a high local viscosity in regions of low average strain rate for the more concentrated solutions and low Reynolds numbers and, therefore, flow laminarization may have occurred.

The preferential damping of tangential and radial Reynolds stresses intensifies turbulence anisotropy and, since $\overline{u'^2}$ is higher than the other two normal components and low levels of turbulence are found in the vicinity of the rear stagnation point, it can be concluded that the main contribution to turbulent production is $\overline{u'v'}\partial U/\partial r$ in the shear layer; this was not the case in the water flow experiment of Taylor & Whitelaw (1984). Although this can improve the usefulness of a K-ϵ turbulence model, the increased turbulent anisotropy can create difficulties and the need for a model separating Reynolds stresses is likely to arise.

The trends observed in the turbulence results resemble those found by Pinho & Whitelaw (1990) in their study of turbulent pipe flow with the same solutions and drag reduction, those of Willmarth, Wei & Lee (1987) in channel flows and those of Koziol & Glowacki (1989) for an axisymmetric jet, both with polymer solutions. The preferential damping of circumferential and radial turbulence is more intense in regions of high normal strain where the flow accelerates or decelerates; that is, the viscosity defined as the ratio of normal stress to normal strain of the polymer solutions increases by at least two orders of magnitude whereas the ratio for Newtonian fluids is constant and equal to three times the viscometric viscosity (Metzner & Metzner 1970). At the same time, strong elongational conditions are also fulfilled by the fact that the flow is turbulent, as demonstrated by Hinch (1977), and the consequent increase in elongational viscosity raises the importance of viscous terms in the mean momentum and turbulent kinetic energy equations by an

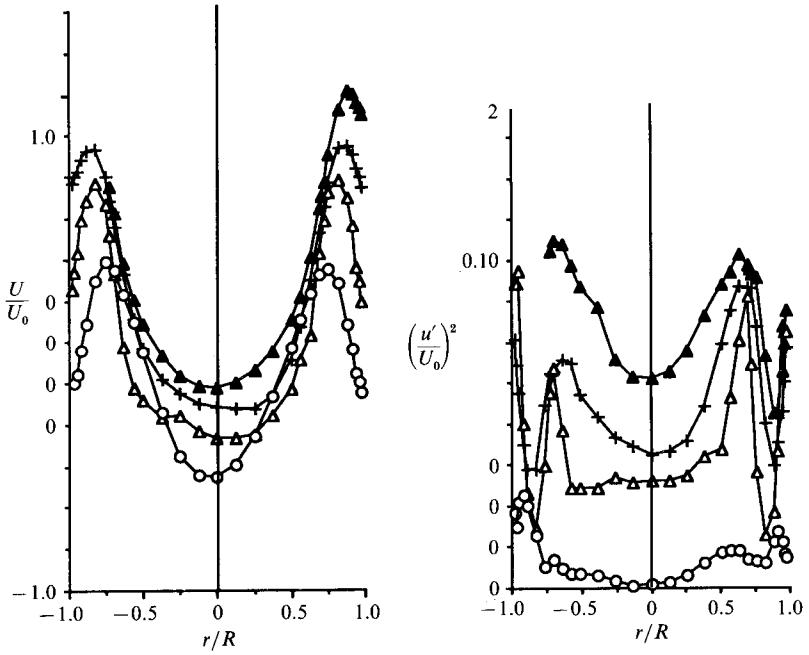

FIGURE 12. Diametral profiles of axial mean velocity and normal Reynolds stress for 0.2% CMC solution at station 1.0D and as a function of Reynolds number. ▲, $Re = 8250$; +$Re = 5520$; △, $Re = 1040$; ○, $Re = 220$.

unknown but certainly non-negligible amount, An order of magnitude analysis of the mean momentum and turbulent kinetic energy equations with an appropriate constitutive equation would show these effects but the complexity of any simple model that is simultaneously able to explain elongational effects and variable viscosity, such as the six-parameter integral model of Tsai & Darby (1978), makes his task difficult and it was not attempted here. Although the present flows have characteristics that can lead to large elongational viscosities, it cannot be concluded that the possible elastic effects are generated downstream of the baffle alone, because the fluid reaches the disk after suffering all the elastic effects associated with drag reduction in the upstream pipe of ninety diameters and there is no evidence that they cease immediately after the influence of a wall disappears. A proper assessment of this effect requires experiments with the baffle located immediately after a settling chamber and convergence.

At Reynolds numbers between 400 and 6000, the Newtonian and non-Newtonian fluids flows are increasingly asymmetric as can be seen in the diametral profiles of axial mean velocity and normal Reynolds stress of figures 11 and 12. The asymmetry had previously been observed by Pinho & Whitelaw (1988) with water and a 0.4% CMC solution for which the effect was larger with the asymmetry preserved at Reynolds numbers higher than 6000. The flow was also unsteady at the centreline and close to the baffle where frequency analysis of the axial velocity detected a frequency (f) of oscillation which, when normalized by the baffle diameter and annular bulk velocity, defined a Strouhal number ($St = fD/U_0$) of 0.094 for Newtonian fluids, 0.079 for 0.2% CMC and, as reported by Pinho & Whitelaw (1988), 0.07 for 0.4% CMC, all values with an uncertainty of 0.005. The energy associated with the oscillations is high, as shown in the large amplitude of the peak at 10.25 Hz of the frequency spectra of figure 13 with 0.2% CMC at a Reynolds number of 3800.

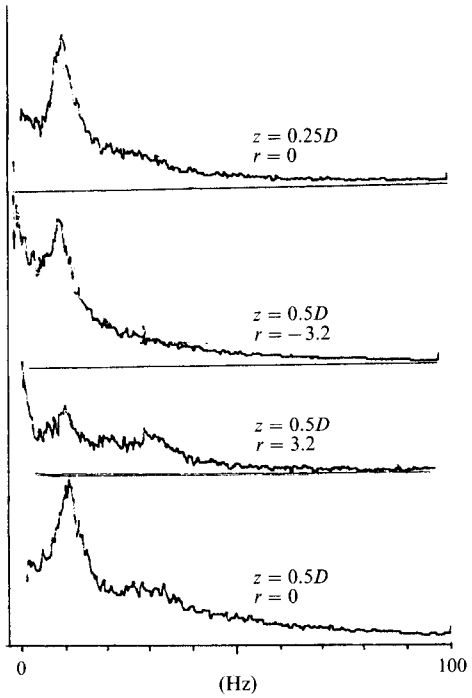

FIGURE 13. Frequency spectra of axial velocity with 0.2% CMC solution at $Re = 3800$.

The preservation of the asymmetric flow at higher Reynolds numbers with the concentrated polymer solutions is similar to the delay in transition from laminar to turbulent flow observed in the pipe flow experiments of Pinho & Whitelaw (1990) with the same fluids, and may be the result of the increase in elongational viscosity due to the elastic effect of molecular stretching. Concentrated polymer solutions are strongly shear-thinning, and the viscosity inside the recirculation bubble is bound to be larger became of the low local average strain rates. The increase of both viscosities contributes to suppress turbulence and, particularly at the smaller scales, leading to the lower frequencies reported above.

The asymmetry seems similar to that found by Cherdron, Durst & Whitelaw (1978) in a sudden expansion at low Reynolds number, and may be the result of the amplification of instabilities shed from the edge of the disk. The asymmetric nature of those instabilities creates an asymmetric flow that interacts with the recirculating flow and a low-frequency periodic oscillation of the bubble is established, similar to the precession of the swirl centre in the recirculation region of a steady open cylinder flow behind an engine valve, Arcoumanis, Hadjiapostolou & Whitelaw (1987). This frequency is two to three times lower than that associated with vortex shedding from the baffle (Calvert 1967), and could not be detected because confinement and the high blockage ratio helped to conceal it, as shown by Sivasegaram & Whitelaw (1985).

Flow unsteadiness is also present below a Rushton impeller in stirred vessel flows at low Reynolds numbers with Newtonian and non-Newtonian fluids (Hockey, Nouri & Pinho 1989). As Reynolds number was increased, the oscillations became less visible because they were smeared by the higher magnitude of turbulence oscillations. From the similarity between the baffle-flow shear layer and the radial discharge jet stream emanating from a Rushton impeller at high Reynolds number, it would not be surprising to observe a deterioration in the quality of micromixing of polymer

solutions due to lower turbulence production in the jet and over the shear layer of the blades, see Pinho & Whitelaw (1990). The suppression of turbulence is expected to be larger in a stirred vessel than in the baffle flow because there are large regions of low mean shear rates far from the impeller, where the high viscosity of a strong shear-thinning fluid may laminarize the flow. Near the blades, large strain rates $(\partial u_i/\partial x_i)$ create the conditions for a rise in elongational viscosity which will also reduce turbulence but the strong three-dimensionality of the mixer flow means that such damping will occur for all stresses.

Although non-Newtonian effects are restricted to low-Reynolds-number flows, their importance should not be ignored because many non-Newtonian fluids have viscosities high enough to prevent fully turbulent flows, as in the present case where, for an annular bulk velocity of around 8 m/s, the maximum Reynolds numbers were 138000 and 7700 with water and 0.4% CMC respectively.

5. Conclusions

The influence of non-Newtonian, shear-thinning, weakly elastic fluids on the flow downstream of a baffle located on the axis of a round duct has been investigated and the results compared with those of Newtonian fluids for a range of concentrations and Reynolds numbers. With Newtonian and non-Newtonian fluids of constant concentration and Reynolds numbers less than 50000, the recirculation bubble length and the normalized recirculation mass flow rate decreased with decrease in Reynolds number, by up to 25% and 15% respectively. Simultaneously, the normal Reynolds stresses decreased with reductions of over 20%. At constant Reynolds numbers, the length of the recirculation bubble increased with CMC concentration and the turbulent kinetic energy decreased, whereas the addition of small amounts of polymer to a Newtonian solvent reduced bubble length and dampened only the tangential and radial components of turbulence. These effects decreased with increasing Reynolds number and the flow of Newtonian and non-Newtonian fluids become similar at Reynolds numbers in excess of 10^5.

Viscous diffusion is not negligible for concentrated polymer solutions but its importance is restricted to low-Reynolds-number flows in regions of low strain rates. With a 0.4% CMC solution at a Reynolds number of 7700, it contributes up to 6% to the largest term of the momentum balance, the pressure gradient term, corresponding to 30% of the turbulent diffusion inside the recirculation bubble and close to the shear layer. Its influence is enlarged if the elongational viscosity is higher than three times the viscometric viscosity. Turbulence suppression is a combined Reynolds-number and polymer-concentration effect which reduces turbulent diffusion, especially inside the recirculation bubble and between the disk and middle bubble planes. The turbulent diffusion in flows of water and 0.4% CMC was reduced by factors of around three close to the baffle and by 30% further downstream.

The asymmetry and unsteadiness of Newtonian and non-Newtonian fluids downstream of the baffle for Reynolds numbers between 400 and 6000 is an aerodynamic effect and the oscillations have a periodicity represented by a Strouhal number of 0.094, 0.079 and 0.07 respectively for Newtonian fluids, the 0.2% and 0.4% CMC solutions. With the more concentrated polymer solutions, the asymmetry was preserved at Reynolds numbers higher than 6000.

The authors are glad to acknowledge financial support from ICI plc and Unilever through a Brite project and would like to thank Dr J. M. Nouri for helpful

discussions. They are also grateful to Professor K. Walters and his team for the guidance and assistance with the rheogoniometer at the University College of Wales, Aberystwyth and to Dr P. Cann of the Tribology Section at Imperial College for equipment and related guidance.

Appendix. Some characteristics of non-Newtonian fluids

The use of laser-Doppler velocimetry to measure the turbulent flow characteristics of shear-thinning fluids in stirred vessels and pipe geometries requires a fluid with low viscosity to allow high Reynolds numbers to be achieved together with an appropriate power-law index, that it maintains its transport characteristics throughout any experiments for a reasonable period of time and that it is sufficiently transparent for the velocity measurements and flow visualisation. In the following paragraphs, these properties of possible fluids are examined after a brief description of the experimental techniques, and this Appendix ends with a summary of the main findings.

Four possible solutions were examined: a 1% by weight solution of Carrageenan 205 Viscarin GP109 in water with 1% by weight of potassium sorbat added to aid conservation; a 0.35% by weight solution of polyacrilic acid Carbopol 941 in a buffered NaOH solution with 0.02% by weight of NaN_3 to prevent bacteriological deterioration; a 3% by weight suspension of silica particles (Aerosil) in a mineral oil (Sirius M85) and a 0.4% by weight aqueous solution of sodium carboxymethil cellulose with 0.07% by weight of the Kathon CG biocide (Rohm & Haas) to prevent bacteriological degradation. First normal stress difference and shear stress in steady shear flows and the complex viscosity in oscillatory flows were obtained with a Weissenberg rheogoniometer, with uncertainties of 2.5% and 5% for shear rates above and below 30 s^{-1}. The mechanical degradation tests were conducted in a pipe rig similar to that of Nouri *et al.* (1987) and a stirred vessel of half the size of that described by Yianneskis *et al* (1987) and the associated changes in viscosity were measured in a cone–plate Ferranti–Shirley viscometer with uncertainties of 5%.

The viscosities of the four solutions are plotted in figure 14 and it can be seen that the Viscarin solution is twice as viscous as the CMC solution and the Carbopol and Aerosil solutions are between 2 and 10 times more viscous, which may preclude turbulent flow. The ratio of the first normal stress difference to shear stress in steady shear flow, the stress ratio, and the ratio of imaginary and real components of complex viscosity in oscillatory flow are summarized in table 5 and indicated some elasticity for the Carbopol solution at deformations below 10 Hz and Viscarin, while the Aerosil suspension and the CMC solution can be considered weakly elastic. These effects were confirmed by the velocity measurements carried out by Larsen & Christensen (1985) in a 1 mm channel flow for the Viscarin solution and it was seen to be opaque for depths of field in excess of 20 mm and therefore unsuitable for the proposed measurements. Other characteristics of the Carbopol solution are the sensitivity of rheology to changes in pH, as Ghorashi & Hirsch (1987) have shown, the poor optical transmissivity at depths of field above 170 mm and the mechanical breakdown of molecules for shear rates over 10^3 s^{-1}, see de Bruijn (1987). This degradation is normal in solutions based in long molecules, and poses a problem of disposal of big quantities of a non-water-based solution (70 l each time). The optical transparency of the Aerosil suspension was good but after several hours in the stirred vessel particles separated and settled down and the increased local viscosity at the bottom of the vessel prevented flow especially in the corners and behind the baffles

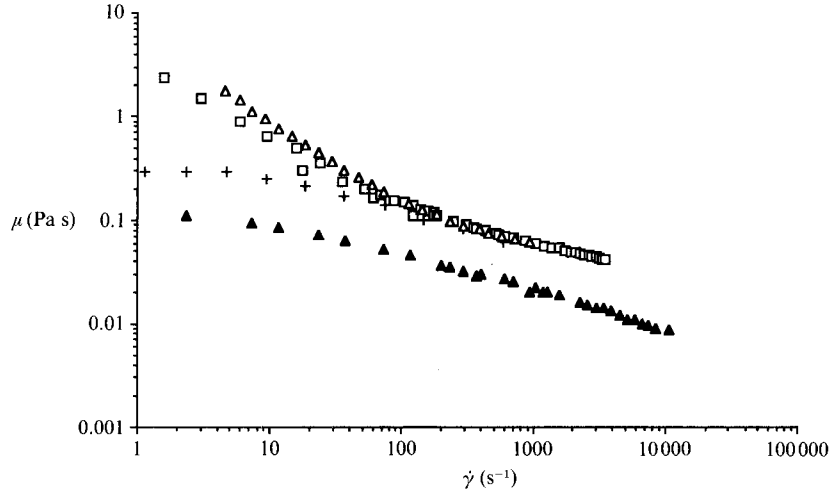

FIGURE 14. Viscosity versus shear rate for □, the Carbopol solution (20 °C); ▲, the CMC solution (25 °C); +, the Viscarin solution (20 °C); and △, the Aerosil suspension (25 °C). Data for Aerosil and Viscarin from K. Walters, W. M. Jones and S. H. Jones (1987, private communication) and for Carbopol from de Bruijn (1987).

Solution	Stress ratio	$\frac{G'}{G''}$
Viscarin	Not available	10 at frequency = 30 Hz 2 at frequency = 1 Hz
Carbopol	0.1 for $1 < \gamma < 20\ s^{-1}$	10 at frequencies < 10 Hz
Aerosil	0.001 at $\gamma = 0.1\ s^{-1}$ 0.2 at $\gamma = 800\ s^{-1}$ 1 at $\gamma = 3{,}000\ s^{-1}$	1 for 1 < frequency < 100 Hz
CMC	Difficult to measure: too low	0.5 to 2 for 0.5 < frequency < 200 Hz

TABLE 5. Some rheological characteristics. Data from de Bruijn (1987).

and remixing could not be achieved. A possible advantage of the suspension is the lack of mechanical degradation since it is based on solid particles rather than long fragile molecules. Optical transparency of the CMC solution was good but mechanical degradation was present; since the solution is water based and the CMC is itself a harmless product, disposal would not constitute a problem.

This study suggested that CMC was the most suitable fluid provided mechanical deterioration does not occur quickly. Figure 15 presents results of viscosity as a function of shear rate and time for the present flow system using a diaphragm and a centrifuged pump. A 10% decrease in the values of the viscosity is observed in the case of the pipe rig after 6 h of shear with the centrifugal pump, 12 h with the double diaphragm pump and 141 h of continuous shear after four days, in the stirred vessel. This suggests the important role of the maximum shear rates in the breakdown of molecules, leading to maximum stresses acting on the molecules.

In conclusion, the CMC solution is the best compromise of the four proposed fluids provided the period of time before a 10% decrease in viscosity occurs is suitable for

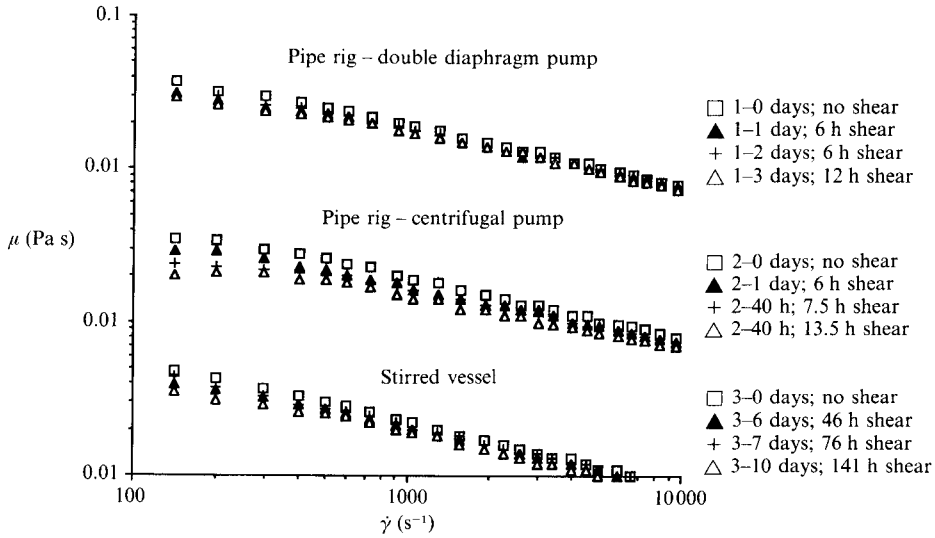

FIGURE 15. Viscosity versus shear rate after being circulated in the rigs. 1- Pipe rig with diaphragm pump; 2-Pipe rig with centrifugal pump; 3-Stirred vessel.

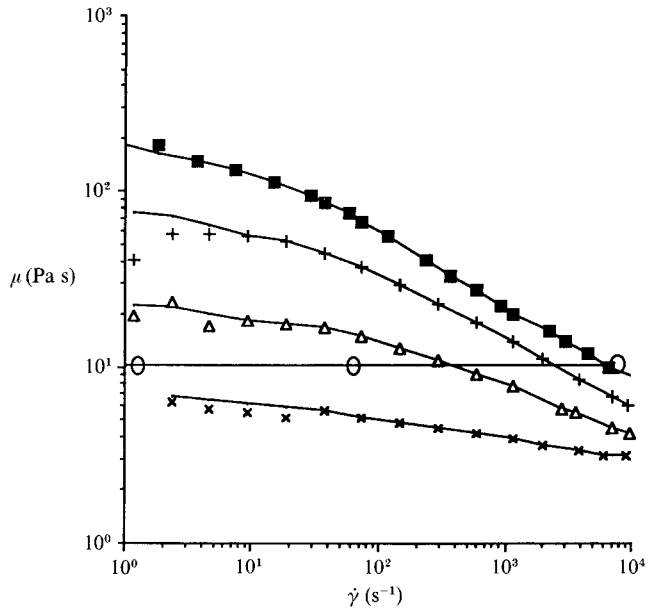

FIGURE 16. Viscosity of CMC and glycerol solutions at 25 °C: ×, 0.1% CMC; △, 0.2% CMC; +, 0.3% CMC; ■, 0.4% CMC; ○, glycerol–water solution.

the experiments, allowing a reasonable number of velocity measurements before discarding the fluid. The Viscarin solution was rejected as opaque at depths of field over 20 mm, the Carbopol solution was too viscous with a low optical transmissivity at depths of field over 170 mm (the stirred vessel used for the velocity measurements has a depth of field of 360 mm) and mechanical degradation occurs with disposal problems. The Aerosil suspension was very viscous but the major setback was the settling of the solid phase over the time.

The dependence of viscosity on shear rate for solutions of 0.3%, 0.2% and 0.1%

Solution	μ_0(Pa s)	λ (s)	n
0.1% CMC	0.007	0.289	0.903
0.2% CMC	0.019	0.034	0.739
0.3% CMC	0.071	0.132	0.688
0.4% CMC	0.167	0.139	0.591

TABLE 6. Simplified Carreau model parameters

CMC is plotted in figure 16, and a least-square fit of the data to a simplified viscosity Carreau model

$$\frac{\mu}{\mu_0} = [1 + (\lambda\dot{\gamma})^2]^{\frac{n-1}{2}} \tag{A 1}$$

was carried out. The parameters are listed in table 6. Since mechanical degradation resistance is known to decrease with a decrease in concentration (Nakano & Minoura 1975), tests were performed on the 0.2% and 0.1% CMC solutions and their properties were also found to be within the 10% limit after 6 h of shear.

REFERENCES

ADACHI, K., YOSHIOKA, N. & SAKAI, K. 1977/78 An investigation of non-Newtonian flow past a sphere. *J. Non-Newtonian Fluid Mech.*, **3**, 107.

ARCOUMANIS, C., HADJIAPOSTOLOU, A. & WHITELAW, J. H. 1987 Swirl center precession in engine flows. *Soc. Automotive Engrs. Paper* 870370.

BARKER, S. J. 1973 Laser Doppler measurements on a round turbulent jet in dilute polymer solutions. *J. Fluid Mech.* **60**, 721.

BERMAN, N. S 1978 Drag reduction by polymers. *Ann. Rev. Fluid Mech.* **10**, 47.

BRUIJN, R. A. DE 1987 Inelastic shear-thinning model liquids. *Unilever Rep.* PA/7306/mk.

CALVERT, J. R. 1967 Experiments on the low speed flow past cones. *J. Fluid Mech.* **27**, 273.

CHERDRON, W., DURST, F. & WHITELAW, J. H. 1978 Asymmetric flows and instabilities in symmetric ducts with sudden expansions. *J. Fluid Mech.* **84**, 13.

DAIRENIEH, I. S. & MCHUGH, A. J. 1985 Viscoelastic fluid flow past a submerged spheroidal body. *J. Non-Newtonian Fluid Mech.* **19**, 81.

FUJII, S., GOMI, M. & EGUCHI, K. 1978 Cold flow tests of a bluff flame stabilizer. *Trans. ASME* I: *J. Fluids Engng.* **100**, 323.

GHORASHI, B. & HIRSCH, D. 1987 Laminar flow of a non-Newtonian fluid in a heated pipe. *Cleveland State University, Chem Engng Rep.*

HINCH, E. J. 1977 Mechanical models of dilute polymer solutions in strong flows. *Phys. Fluids Suppl.* **20** S22.

HOCKEY, R., NOURI, J. M. & PINHO, F. T. 1989 Flow visualization of Newtonian and non-Newtonian fluids in a stirred reactor. In *5th Intl Symp. on Flow Visualization, Praha, CSSR, August 21–25.*

KWADE, M. 1982 Beeinflussung der Turbulenzstruktur in der Ebenen Mischungsschicht zweier Ströme durch Polymerzusätze. *Rheol. Acta* **21**, 120.

KOZIOL, K. & GLOWACKI, P. 1989 Turbulent jets of dilute polymer solutions. *J. Non-Newtonian Fluid Mech.* **32**, 311.

LARSEN, P. S. & CHRISTENSEN, E. M. 1985 Velocity distributions of water and viscarin solutions in straight channel. Technical University of Denmark, Dept of Fluid Mechanics. Rep. AFM 85-05.

MENA, B. MANERO, O. & LEAL, L. G. 1987 The influence of rheological properties on the slow flow past spheres. *J. of Non-Newtonian Fluid Mech.* **26**, 247.

METZNER, A. B. & METZNER, A. P. 1970 Stress levels in rapid extensional flows of polymeric fluids. *Rheol. Acta* **9**, 174.

NAKANO, A. & MINOURA, Y. 1975 Effects of solvent and concentration on scission of polymers at high speed stirring. *J. Appl. Polymer Sci.*, **19**, 2119.

NOURI, J. M. 1988 Single and two-phase flows in ducts and stirred reactors. Ph.D. thesis, University of London.

NOURI, J. M. & WHITELAW, J. H. & YIANNESKIS, M. 1987 Particle motion and turbulence in dense two-phase flows. *Intl. J. Multiphase Flow* **13**, 729.

PINHO, F. T. & WHITELAW, J. H. 1988 Flow characteristics of a non-Newtonian fluid. In *4th Intl Symp. on Applications of Laser Anemometry to Fluid Mech., 11–14 July 1988, Lisbon* (ed. D. F. G. Durao, R. J. Adrian, T. Asanuma, F. Durst & J. H. Whitelaw), *Paper* 1.23.

PINHO, F. T. & WHITELAW, J. H. 1990 Flow of non-Newtonian fluids in a pipe. *J. Non-Newtonian Fluid Mech.* **34**, 129.

SIVASEGARAM, S. & WHITELAW, J. H. 1985 Vortex shedding in disk stabilised flames. *Internal Rep. FS/85/01.* Imperial College, London.

TAYLOR, A. M. K. P. & WHITELAW, J. H. 1984 Velocity characteristics in the turbulent near wakes of confined axisymmetric bluff bodies. *J. Fluid Mech.* **139**, 391.

TSAI, C. F. & DARBY, R. 1978 Non Linear viscoelastic properties of very dilute drag reducing polymer solutions. *J. Rheol.* **22**, 219.

WHITE, D. A. 1967 Velocity measurements in axisymmetric jets of dilute polymer solutions. *J. Fluid Mech.* **28**, 195.

WILLMARTH, W. W., WEI, T. & LEE, C. O. 1987 Laser anemometer measurements in turbulent channel flow with drag reducing polymer additives. *Phys. Fluids* **30**, 933.

YIANNESKIS, M., POPIOLEK, Z. & WHITELAW, J. H. 1987 An experimental study of the steady and unsteady flow characteristics of stirred reactors. *J. Fluid Mech.* **175**, 537.